The Polish UV Satellite – UVSat: preliminary scientific programs for spectroscopy.

B. Czerny[1,2], M. Drahus[3], P. Guzik[3], B. Handzlik[3], K. Hryniewicz[2], J. Mikołajewska[2], S. Mochanacki[2,4], T. Mrozek[5,6], G. Pietrzyński[2], A. Różańska[2], M. J. Sarna[2], M. Stęślicki[5], J. Sylwester[5], W. Waniak[3]

1 Center for Theoretical Physics, PAS
2 Nicolaus Copernicus Astronomical Center, PAS
3 Astronomical Observatory, Jagiellonian University
4 University of Toronto
5 Space Research Center, Solar Physics Division, PAS
6 Astronomical Institute, University of Wroclaw

1. Scientific Requirements: UV Spectroscopy

1.1 A Proposed Ultraviolet Spectrometer for the Polish UV Satellite.

Concept (The scientific justification, programs, etc. will be covered in a separate paper).
The most capable and productive general purpose UV spectrometers flown to date are the International Ultraviolet Explorer (1977-1996; 45 cm aperture telescope; Boggess et al. 1978)), and the Cosmic Origins Spectrograph (COS; 2009- ; Green et al., 2012) and Imaging Spectrograph Instrument (STIS; 1999-2004, 2009- ; Woodgate et al. 1998) on the Hubble Space Telescope (HST; 260 cm aperture). A low resolution spectrograph was flown on the UV imaging satellite GALEX (Siegmund et al. 2004). A very small spectrograph, the Colorado Ultraviolet Transit Experiment (CUTE; Fleming et al. 2018) is being built, with launch planned for 2020. The concept presented here draws on these designs. Numerous other UV spectrometers have flown or are being designed, but they generally are more specialized or not as relevant.

Reflecting the interests of Polish astronomers as presented later in this proposal, we consider two possible telescope aperture sizes (30 cm and 50 cm), with FUV (115 – 220 nm) capability, at resolution (R = 3000). This basically would cover all of our science requirements of potential investigators and attainable on a small platform.

At this stage, we leave alone the detailed design of the spectrograph. The development of ion etched holographic gratings which also act as aberration-corrected focusing elements allows great simplification over the traditional designs such as in IUE. These can be described as Rowland circles modified for flat detectors, and we assume that is the layout to be used on UVSat. We illustrate CUTE below:

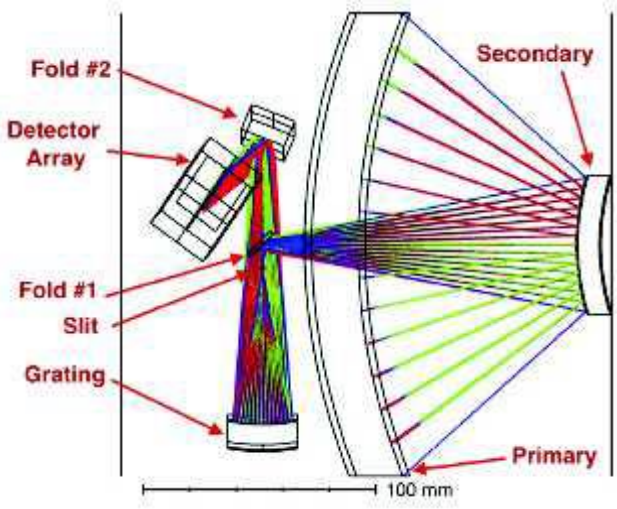

Fig. 1.1. CUTE spectrograph schematic. This is a raytrace diagram of the 20cm x 8 cm aperture telescope, with dispersion direction out of the page. Spectral coverage 251.5 – 333.5 nm. Resolution ~ 3000. (Fleming et al. 2018)

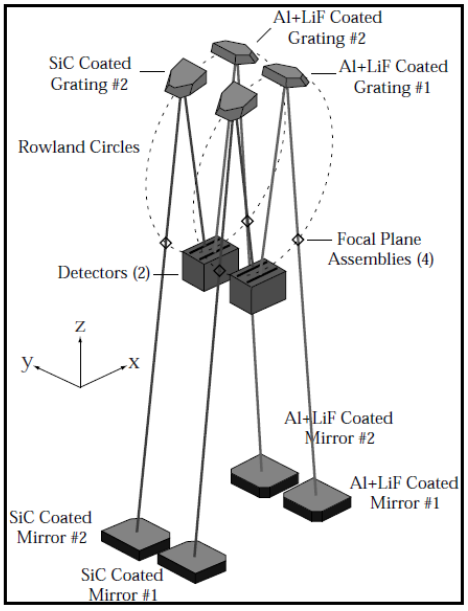

Fig. 1.2. FUSE optical design, for shorter wavelengths and higher resolution (Sahnow et al. 2000), in this case observing in four narrow bands within the range of 90 to 119 nm. Each channel consisted of one telescope mirror and one aberration-corrected spherical grating which acted in place of the usual collimator, grating and camera elements. A focal plane assembly provided as apertures or slits.

The detectors were opaque KBr photocathode microchannel plates (MCP) with helical double delay line anodes (Siegmund et al. 1997), giving photon counting with a quantum efficiency of 40% at 115 nm and dark count rates of less than 0.5 event/cm^2/sec.

Modern gratings in the UV can attain up to 65% efficiency and mirror reflectivity of 90% can be safely assumed (Fleming et al. 2018). In the computations below, we conservatively assume a telescope efficiency of 80% and a spectrograph transmittance of 60%.

1.2 Detectors

We leave alone the choice of detector, noting however that solid state detectors now work well down to about 150 nm. This question has been studied in earlier work on UVSAT, and also for the Canadian CASTOR proposal (Scott et al. 2014). However, it will probably be necessary to use an intensifier photon counting detector as in FUSE and GALEX, a well proven and mature

technology, to reach the scientifically valuable region between 115 and 150 nm. The MCPs typically have 10 micron pores pitched at 12.5 microns, and centroiding of photon events leads to a FWHM of about 20 microns in the favored X dispersion direction (Siegmund et al. 1997). Here we shall assume such a detector. A solid state detector, if it could work below 150 nm, would have higher quantum efficiency and greater dynamic range but would require greater cooling. The intensified photon counting detector can also made Sun-blind more easily.

In the calculations, a value of 0.4 is assumed for the quantum efficiency and 0.5 event/cm^2/sec for dark current. The effective quantum efficiency can be expected to decline by about 20% per year. Pulse height discrimination allows the dark current level to be maintained despite the effects of radiation in orbit (Sahnow et al. 2000). We assume that the resolution is matched to the detector so that one resolution element is 20 x 60 microns (ibid.), or 12 pseudo-pixels each of 10 x 10 microns. The dark current would then be 6×10^{-6} events/sec/resolution element. The sky background in the FUV is conservatively taken as 600 photons cm^{-1} s^{-1} sr^{-1} $Å^{-1}$ (cf. Murthy et al. 2010). This would require a detector of length approximately 42 mm to give the required 4200 pseudopixels each of 10 microns over the 105 nm bandwidth, with a plate scale of ~ 5 arc seconds per resolution element (for 30 cm aperture telescope), and ~ 3 arc seconds for the 50 cm telescope but identical spectrograph with 50 mm grating diameter. A detector of 42 mm length is quite large, although FUSE used segments of 90 mm x10 mm.

Table 1.1. Assumed parameters for expected signal calculations, for two apertures. (* : The same spectrograph in each case, with only projected slit size changing).

Aperture	30 , 50 cm
Central obstruction diameter	9 , 15 cm
Telescope Rayleigh limit @ 150 nm	0.14 , 0.08 arc sec
Nominal f/ratio (telescope and spectrograph)	3.0
Nominal spectrograph grating (beam) size	50 mm
Nominal slit width projected on sky *	5 , 3 arc sec
Slit width	22 microns
Grating spatial frequency	2565 lines/mm
Dispersion angle	12.4 deg
Projected slit width	2 pseudopixels
Maximum count rate/pseudopixel	10 events/sec
Assumed telescope optical efficiency	0.8
Central wavelength, bandpass	167 nm (105 nm coverage)
Flux at ST mag.=0 at all wavelengths	3.63×10^{-9} erg s^{-1} cm^{-2} A^{-1}
Assumed spectrograph optical efficiency	0.6
Resolution R	3000
Quantum efficiency	0.4
Read noise	0 (photon counter)
Operating temperature	0 C (nominal)
Dark current	0.5 $electrons^{-1}$ cm^{-2} sec^{-1}
Project star image length	3 pseudopixels
Assumed PSF FWHM	2 pseudopixels
Assumed sky brightness in band	1.4×10^{-8} photons s^{-1} $arcsec^{-2}$ A^{-1}
Assumed pseudopixel size	10 microns

A photon counting FUV detector in the moderate resolution configuration we propose has three very useful features:

- The slit can be quite long, allowing observation of extended objects such as nebulae and comets, which typically have many interesting lines in the FUV. The nominal design presented here would allow for a slit length of many minutes of arc, depending on how wide a field is allowed by the telescope optics.

- The locations and times of individual photon events can be recorded given sufficient data storage space, which is not difficult with modern memory technology. This allows for a photon arrival time resolution of milliseconds to microseconds, depending on the detector technology chosen. Correlation of star tracking spacecraft positions with photon position will allow correction for star image wander across and along the slit, allowing for improved resolution and radial velocity stability. The recorded photon times will also allow correction for Doppler movement due to spacecraft orbital motion, again improving spectral resolution and radial velocity accuracy. On top of this, the high time resolution will allow the study of very rapid events, which are particularly common in cases of material accreting onto degenerate objects such as white dwarfs, neutron stars and black holes.

- A custom star tracker/guider camera can also be used to simultaneously provide precise visible light photometry of the star being observed by the FUV spectrometer, as well as other stars in its field. Since the slit will be quite wide, the flux recorded by the spectrometer will provide calibrated spectral energy distributions and hence FUV photometry. This dual band observing mode will be a unique feature of UVSAT, and will address several important scientific questions. The time resolution of a tracking CCD or CID would be some tenths of a second, quite useful alongside the very high time resolution of the spectrometer.

The integration times are calculated for given as a function of ST monochromatic magnitude for signal to noise ratios of 10, 20 and 50, at wavelength 167 nm, for resolution of R=3000 for telescope apertures 30 and 50 cm (spanning what is possible on a microsat platform) and a single spectrograph with 50mm beam (grating) diameter. Projected slit widths of 5 and 3 arc seconds respectively will produce the desired resolution for each telescope size. The spectrograph numbers will all be juggled to optimize the final system, but the response will remain much the same.

The calculations for S/N=10, 20 and 50 are shown in Table 1.2. For a 30 cm telescope, S/N of 50 can be reached in 20 minutes at ST magnitude of 10. A 50 cm aperture telescope allows observations of stars about one magnitude fainter to the same S/N ratio in the same integration time. In Figures 1.3 and 1.4 are shown the 30 cm and 50 cm integration times for given ST magnitude at 167 nm.

Table 1.2. Far Ultraviolet (FUV) exposure times to produce given S/N per resolution element, for 30cm and 50cm apertures, resolution = 3000. No consideration of maximum count rates has been taken, but is likely to be around ST = 8-9 (in the FUV), assuming maximum rates of around 10 photon events/sec/pore.

Object	30 cm Telescope	50 cm Telescope

ST	Star signal	S/N	S/N	S/N	Star signal	S/N	S/N	S/N
magnitude	pe/res.el/s	10	20	50	pe/res.el/s	10	20	50
0	20980	0.005	0.019	0.119	58278	0.002	0.007	0.043
1	8352	0.012	0.048	0.299	23201	0.004	0.017	0.108
2	3325	0.03	0.12	0.75	9236	0.011	0.043	0.271
3	1324	0.08	0.30	1.89	3677	0.03	0.11	0.68
4	527	0.19	0.76	4.74	1464	0.07	0.27	1.71
5	210	0.5	1.9	11.9	583	0.17	0.69	4.29
6	84	1.2	4.8	29.9	232	0.4	1.7	10.8
7	33	3.0	12.0	75.2	92	1.1	4.3	27.1
8	13	8	30	189	37	2.7	10.9	68.0
9	5	19	76	474	15	7	27	171
10	2.10	48	191	1192	6	17	69	429
11	0.84	120	479	2993	2.32	43	172	1078
12	0.33	301	1203	7520	0.92	108	433	2707
13	0.13	756	3023	18895	0.37	272	1088	6800
14	0.053	1900	7600	47499	0.15	683	2734	17086
15	0.021	4782	19127	119543	0.058	1718	6872	42948
16	0.008	12069	48276	301725	0.023	4323	17291	108067
17	0.003	30681	22725	767034	0.009	10905	43622	272636
18	0.001	79373	317493	1984331	0.004	27692	110768	692299

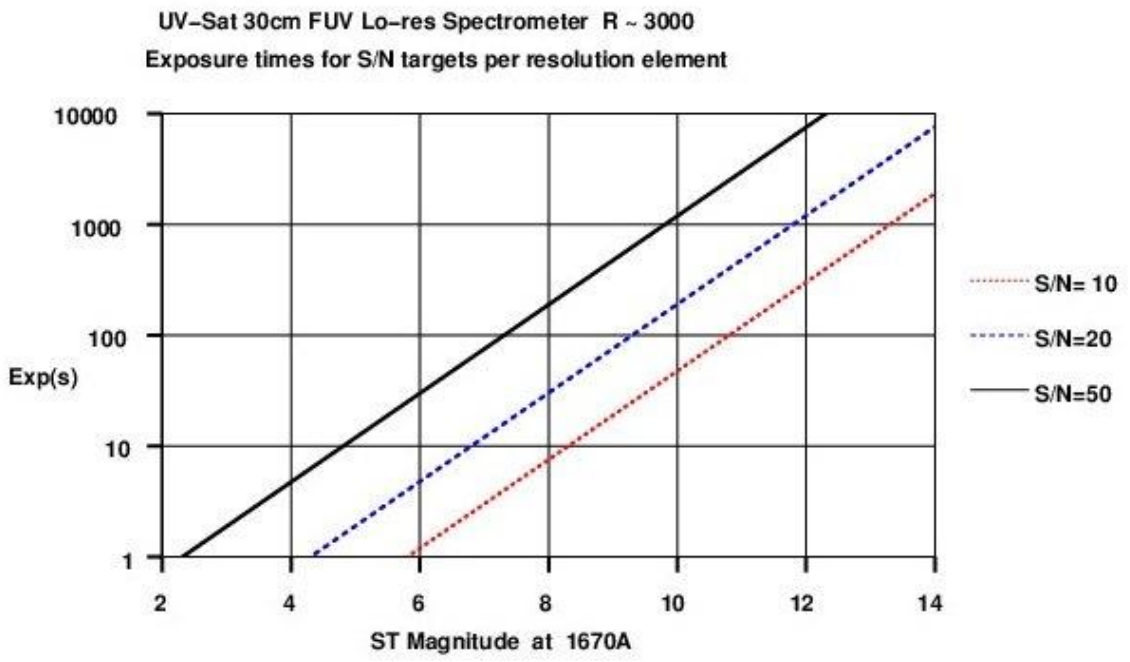

Fig. 1.3. Integration times for 30 cm aperture telescope with resolution 3000 spectrograph in the FUV. Spectra with S/N ~ 50 can be observed in about 20 minutes at 10th ST magnitude.

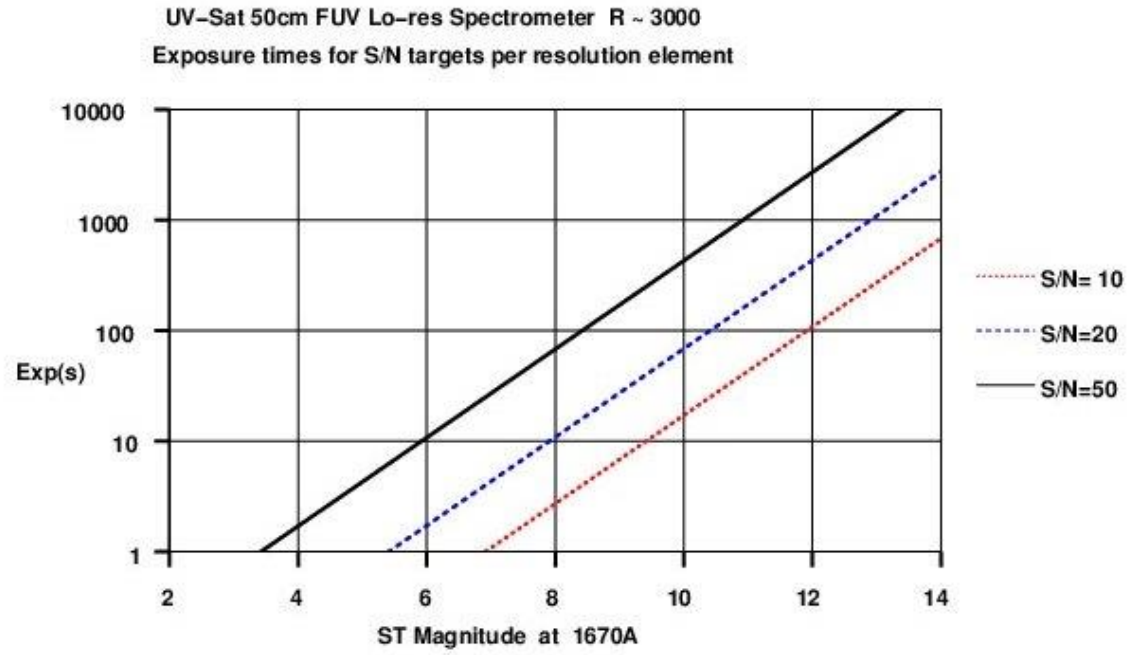

Fig. 1.4. Integration times for 50 cm aperture telescope with resolution 3000 spectrograph in the FUV. Spectra with S/N ~ 50 can be observed in about 20 minutes at 11th ST magnitude.

2. UV Space Spectroscopic Missions

The spectroscopic parts of the earlier mentioned missions are discussed below; refer to the photometric section for full details on these missions.

2.1 Currently operating

2.1.1 HST:

Cosmic Origins Spectrograph (COS): Cos has NUV and FUV channels as noted elsewhere, with resolution 1500 to 24000. The design of this spectrograph is highly relevant to UVSAT (Green et al. 2012).

Space Telescope Imaging Spectrograph (STIS): The NUV and FUV channels have resolutions ranging from 26 to 200 000. The Hubble Space Telescope is expected to be in operation until about 2020 (see: http://www.space.com/29206-how-will-hubble-space-telescope-die.html). HST has many mission purposes, and UV spectroscopy occupies only a fraction of its time, although COS and STIS are very capable.

2.1.2 XMM-Newton

The spectrograph operates only in the X-ray region (0.35-2.5 Kev).

2.1.3 Hisaki (SPRINT-A)-EXCEED

The EXCEED spectrograph operates in the EUV region (54-148nm) at 0.3-0.5nm resolution (R ~ 300). Hisaki was launched in 2014, so should have considerable life left.

2.1.4 ASTROSAT - UVIT

UVIT consists of two co-aligned 38cm telescopes that provide ~1 arsec resolution imaging over 28 arcmin fields, in FUV, NUV, and Visible bands simultaneously (Hutchings 2014). It was launched in 2015. It is important as a relatively modern implementation of compact UV detectors, although it does not have spectroscopic capability.

2.2 Planned missions

2.2.1 EUVO (European Ultraviolet Visible Observatory) and ATLAST-8

These are European and American proposals respectively (Gomez de Castro et al. 2014, Stahl et al. 2010), for 8-metre aperture UV/optical space telescopes. These missions would be far in the future if ever funded, a third generation large space telescope following HST and JWST.

2.2.2 HORUS/ THEIA /HabEx/ LUVOIR

This is a series of American studies for a 2.4 metre class UV/visible telescope. P. Scowen (private communication) reports that a smaller version may be proposed as a Probe-class mission. There is no development path toward an actual flight yet.

2.2.3 WSO-UV (Spektr-UV)

This will be a 1.7 metre, f/10 telescope including an imaging and slit less spectrograph (ISSIS) and a triple spectrograph system WUVS with resolution in the range 1000 to 50 000 in the NUV and FUV bands. As reported elsewhere (Sachkov et al. 2016) it may be launched in 2021.

Table 1. Main characteristics of the UVPS, VUVPS, and Long Slit (LSS) channels of the spectrograph of WSO-UV

Channel	Wavelength range	Resolving power
UVPS	174 – 304 nm	55.000
VUVPS	115 – 176 nm	
LSS	115 – 310 nm	1.000
Spatial	0.5 – 1".0	

2.2.4 GESE (Galaxy Evolution Spectroscopic Explorer)

This is a proposal, still in early stages, for a 1.5 metre UV-O-IR multi-object wide-field (0.3 degree) telescope principally for NUV spectroscopy of many galaxies at once at low resolution (R ~ 400). It would be a lead into the very large EUVO space observatory.

2.2.5 UVMag/ARAGO

This is an advanced proposal for a 1.3 metre telescope with high-resolution (R ~ 25 000 - 35 000) spectropolarimeter, in FUV, NUV and Visible. Funding is being sought and the craft would probably fly around 2030 and be located at the Earth-Sun L2 point. Its significance is that it would measure magnetic fields.

2.2.6 CUTE (Colorao Ultraviolet Transit Experiment)

This nanosat-sized satellite is described in section 1 (Fleming et al. 2018). It uses a 20 x 8 cm rectangular aperture telescope; its design is higly relevant to UVSAT.

2.3 Discussion

After HST ceases operation around 2020, the only planned FUV and NUV spectrographic satellite planned to be flying is WSO-Spektr-UV. No other project is fully funded at this stage, and none is likely to fly before 2015 or even 2030.

There is an important niche, especially in the years 2020-2025, to be filled by even a small space telescope equipped with a spectrograph with moderate resolution especially in the FUV passband observing one stellar-like object at a time. UVSat can have the unique capability of simultaneously performing high precision visible and UV photometry and UV spectroscopy in the same field.

3. Preliminary Overview of Scientific Programs

3.1 Introduction

A number of Polish astronomers (see attached documents) have expressed an interest in having a space-based UV spectrograph. In particular, the region of 1000-2000 Å attracts interest, with 2000-3200 Å of lesser but significant interest. Resolutions of 20,000 - 60,000 and of 2000 have been requested.

3.2 Interacting binaries and transients involving hot sources.

Satellite UV spectroscopy (~1200-3000 A) is of paramount importance to investigate hot stars, especially those with winds, interacting binaries, and any kind of transients. This is due to the presence of many strong, astrophysically important transitions present in this range. In particular, these are strong resonance lines of CIV, SiIV, NV, AlII, MgII, inter-combination lines: NIV], NIII], CIII], SiIII], OVI] as well as forbidden: [NeIV], [NeV], [Mg V], [SIV] . Majority of these transitions are in the short (~1200-2000 A) UV range.

The study of astrophysical transients, over all wavelengths, time and distance scales in the Universe, has entered a new era with the establishment of a number of ground- and space-based facilities, used in both detection and follow up programs. There is growing interest amongst Polish astronomical community to study astrophysical transients across a variety of object classes, especially given the development of new ground-based facilities/surveys in the near future (e.g. MeerKAT, LSST and SKA) the opportunity to study the transient Universe will be unprecedented. However, the satellite UV spectroscopy seems to be a niche that the proposed UVSAT project could fill up. Even with a relatively small aperture a lot of interesting science could be done provided that:

- the satellite will be able to make long, uninterrupted, exposures (~10000 sec) of faint objects or repeated exposures of variable, evolving objects;
- it will be possible to schedule observations of newly discovered transient sources on short notice (hours but even a few days is still ok for many kinds of targets);
- it will be suitable for variability surveys – multi-year project.

Among transients that would particularly benefit from UV spectroscopy are:

- binaries involving accreting whited dwarfs (WDs) , e.g., cataclysmic variables (CVs), symbiotic stars (SySt), and super soft X-ray sources (SSXS);
- X-ray/γ-ray transients, including low and high mass X-ray binaries (LMXBs and HMXBs) and gamma ray binaries
- novae
- bright supernovae (SN)

Examples of possible projects are given below. In this study we adopted the ST MAG system, i.e., $m_\lambda = -2.5 \log_{10} F_\lambda - 21.1$, where F_λ is the spectral flux density per unit wavelength of a source at the top of the Earth's atmosphere in units of erg s^{-1} cm^{-2} A^{-1}.

3.3 Novae

About 40 classical novae (CNe) per year are expected in MW but not all observed, e.g., in 2018, so far 9 novae have been detected in MW (21.04.2018) and one in the LMC (which has turned out

to be a recurrent nova). A few CNe/yr are expected in the MCs; e.g., the nova rates of 2.4 ± 0.8 per year (LMC) and 0.9 ± 0.4 per year (SMC) were derived from OGLE data (Mróz et al. 2016).

CVs are among the most common interacting binaries in which a red/brown dwarf donor (majority), subgiant or giant donor transfers material to WD companion. The accretion of H-rich material leads to various outburst phenomena among the most spectacular are thermonuclear nova (CNe) explosions. Nova explosions provide large enrichments of interstellar medium in CNO as well as Ne, Na, Al and other intermediate-mass elements, and their study is essential to understand the Galactic nucleosynthesis including the 'life' elements. Furthermore, CO novae (i.e. those occurring on CO WDs) the main ^{7}Li factories in galaxies and they can produce all (and even more) Li observed in excess of that predicted by the Bing Bang nucleosynthesis (e.g. Molaro et al. 2016). Since novae are explosive phenomena, each of them is unique and worth detailed study.

UV observations of novae in outburst allow to determine chemical abundances, masses and velocities of the ejecta, mass loss rates, and continuum flux distribution. Exemplary UV spectra taken during nebular phase are shown in Fig. 3.1. These spectra reveal wealth of emission lines, in particular, in addition to HeII lines, strong resonance lines of CIV, SiIV, NV , intercombination lines of NIV], NIII], OIII], CIII] and SiIII. Because many elements are only observable in the UV (among these the most important are C and Si), it is possible to determine abundances for many more elements than it is possible with only optical data. In addition, only with UV spectra one can unambiguously distinguish between CN outburst occurring on CO and ONeMg white dwarf – see Fig. 3.1.

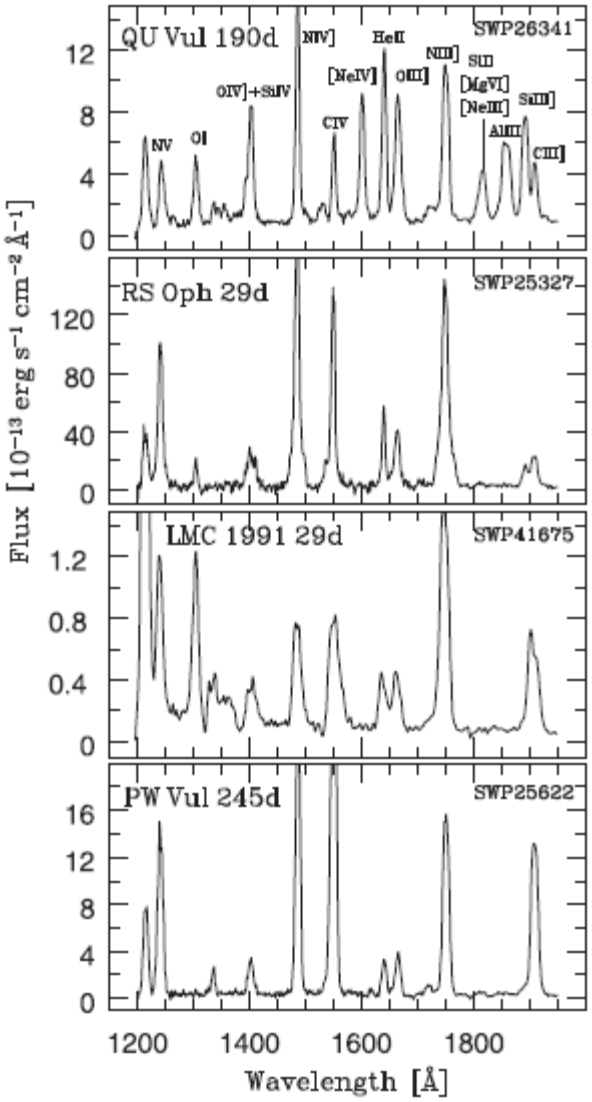

Fig. 3.1. Comparison of IUE low-resolution spectrum of RS Oph, the ONeMg nova QU Vul, and two CO novae LMC 1991 (very fast) and PW Vul (from Mikołajewska & Shara 2017).

CNe are very luminous objects, and even UVSAT would easily observe them in the Magellanic Clouds (e.g., their ST mag m_{1500}~ 10-11 in MCs) and the brightest (and fastest) novae would be detectable in the Local Group og Galaxies. Note that in the case of these distant novae, just the presence or absence of some lines (AlII, [NeIV]) permit to distinguish between CO and ONeMg novae.

3.4 SN and their remnants

Another class of transients are all kinds of supernovae (SN), and one should expect that a few bright (nearby) SN will happen.

UV spectroscopy provide much more leverage for interpretation of physical conditions, abundances and the physical processes at work in the shocked gas than do optical spectra alone.
The highest ionization lines in the optical SNR spectra are usually those of [OIII] , [NeIII] and [NII] that are formed in a region of 20000 to 40000 K.
UV range contains lines of many higher ionization lines such as OVI, CIV, SiIV and NV, which sample temperatures up to 200000 K or more. Just the presence of absence of these lines permit a much stricter interpretation of the peak post-shock temperature, and thus the shock velocity.
UV range is also crucial to derive the spectral energy distribution (SED) which, e.g., show strong departures from black body in UV range, especially in SN I and Ia) , and to derive abundances, e.g. N/C (SN II).

3.5 Symbiotic stars and super soft X-ray sources

Currently, about 300 symbiotic stars (SySt) are known in MW and about 20 in MCs, however much more are expected to be detected in the coming years by ongoing systematic surveys for these objects.

SySt and other binaries with hot luminous components (e.g., SSXS) have luminosities comparable to nova during the plateau phase because most of classical SySt (Fig. 3.2) and likely all SSXS contain WDs more or less steadily burning H-rich material as it is accreted. Their study is very important to understand the growth of the WD mass towards Chandrasekhar limit, and the evolution towards Supernova type Ia (SN Ia) explosions (e.g., DiStefano 2010, Mikołajewska 2013). These systems show variations in continuum flux, line profiles, and luminosity with time due to their orbital motion and long term evolution and activity. UV allows to determine whether the changes are due to variations in mass loss, mass accretion or the compact component temperature.

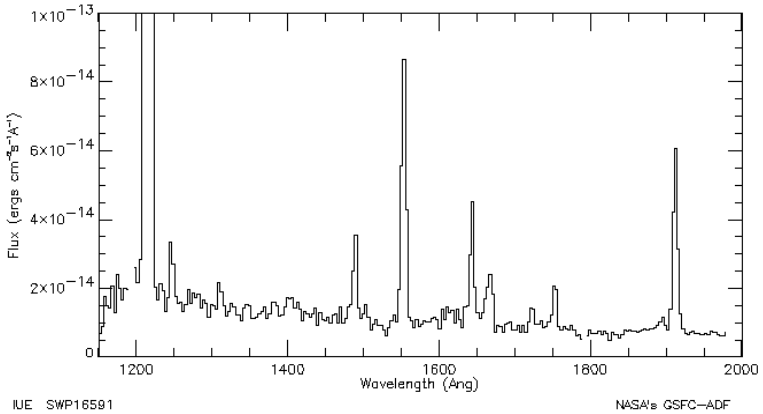

Fig. 3.2. IUE spectrum of SySt LMC S63.

3.6 Hot evolved stars with winds

Evolved hot stars, Wolf-Rayet (WR) stars, luminous blue variables (LBV) and OB stars are very important testbed for massive star evolution. There are bright and could be easily observed even with a small aperture satellite. E.g., typical ST magnitude at 1500 A for WR stars in the MCs are m_{1500}~8-10. With longer exposure times (~10000 sec) they could be also reached in the Local Galaxy Group (LGG). There are about a few hundred known WRs in MW, MCs and LGG. Even low resolution spectroscopy will provide important insights into the velocity and ionization characteristics, while high resolution mode (for the brightest objects) will give more detailed insights in their wind structure.

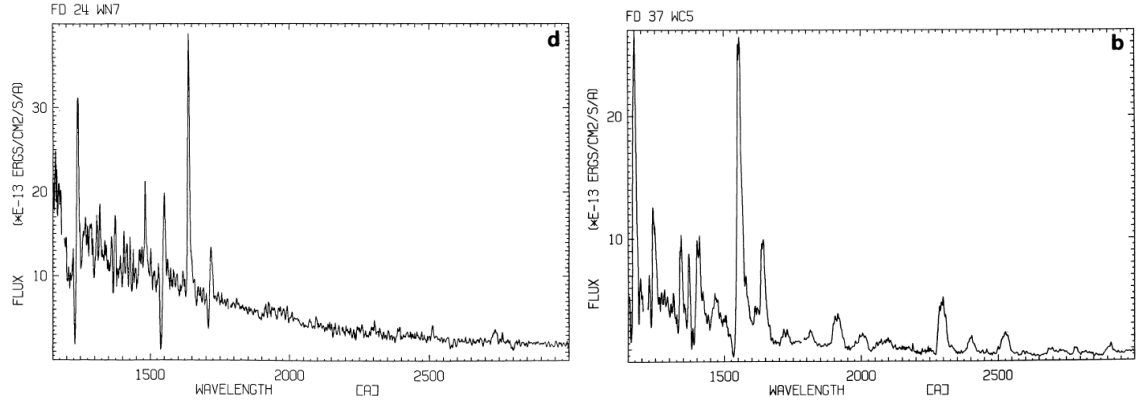

Fig. 3.3. Exemplary UV spectra of WR stars in the LMC): FW 24 (WN7; m_{1500}=8.7) – left, and FD 37 (WC5; m_{1500}=10.1) – right (from Smith & Willis 1993).

A lot of work done but variability, especially due to their possible binarity (according to present view up to ~90% are in binaries), binary interactions as well as intrinsic variability remains poorly studied. Thus systematic monitoring of these objects, especially those in MCs, M33 and M31, would be very important because of their known distances (and possibility to derive accurately all distance-dependent characteristics) and significantly different metallicities of these galaxies (from nearly solar – M31 though moderately low – LMC to very low M33 and SMC) and can results in many interesting discoveries.

3.7 Contact Binary Stars

An unresolved question regarding W UMa-type contact binaries is whether the less massive components in cooler systems (spectral type G0 or later) are actually cooler than the more massive components or simply have fewer spots. Nearly all current publications assume the hotter secondary model, yet very detailed fitting to VW Cep with spotfitting suggest that Lucy's model (Lucy 1968a,b) correctly predicts the temperature difference and the observed "excess" is due to spots (Hendry and Mochnacki 2000). UV observations of W Uma itself (Eaton, Wu and Rucinski 1980) with the ANS satellite indicated that there was no temperature excess on the secondary and that spots would account for the excess apparent brightness of the less massive component. Observations of several contact binaries using UV spectrophotometry combined with simultaneous photometric measurement in visible light will resolve this important question of the "W-effect" once and for all. There are many otherwise well studied contact binaries between 7th and 12th magnitudes around the sky which can be used for this.

One of the most important contact binaries is the extreme mass ratio object AW Uma, discovered by Paczyński (1964) and first fitted in detail by Mochnacki and Doughty (1972). The photometry strongly agrees with Lucy's common envelope "over contact" model and a mass ratio of 0.07-0.08 (Eaton 2016). Very detailed spectroscopy by Pribulla and Rucinski (2008) and Rucinski (2015) questions the photometrically-derived model, indicating that there is a stream between components which are not joined in a common envelope, with a mass ratio of 0.10. In this case, far UV spectroscope will easily detect any stream or disk, and resolve this very important and contentious paradox concerning Paczyński's Star. Several other objects similar to AW Uma will be accessible to UVSAT.

4. Classical Cepheids as tools of distance estimator

Introduction: Classical Cepheid stars have been considered for more than a century as reliable tools to estimate distances in the universe thanks to their Period-Luminosity (PL) relationship. This relation is one of the primary tools of cosmology, the first step in calibrating the extragalactic distance scale (see e.g. Riess et al. 2011). As they overlap with secondary distance indicators, the contribution of the Cepheids distances should not be underestimated. Moreover, Cepheids are also powerful astrophysical laboratories, providing fundamental clues for studying the pulsation and evolution of intermediate-mass stars. The mass is the most fundamental parameter for a star, but this parameter is usually hard to measure. Knowing this variable for a Cepheid is even more critical since the first hydrodynamic calculations produced smaller masses than evolutionary tracks (Stobie 1969). When a Cepheid is in a binary system, we can investigate the age and evolution of the Cepheid, estimate its mass and distance, and constrain theoretical models.

Why ultraviolet spectroscopy? Measuring the mass of a star is possible if the star belongs to a binary system. In addition, the system has to be resolved both spatially and spectrally, i.e. the binary needs to be both visual (or astrometric) and double-line spectroscopic. Otherwise, mass and distance are degenerate parameters, unless the system is eclipsing. In the case of Cepheids, there is no truly direct parallax measurement better than 4 %, and the average accuracy of Milky Way parallaxes is 8 %, which already limits the mass accuracy. We have currently two problems in the case of binary Cepheids: 1) most of the known companions are located too close to the Cepheid (< 40 mas) to be observed with an 8-meter class telescope, and 2) the Cepheid brightness outshines its main-sequence companion from optical wavelengths. We recently solved the first point using interferometry which provides angular resolution down to ~ 1 mas. For V1334 Cyg Ab. An astrometric orbit is being constructed using both northern and southern interferometers (see e.g. Gallenne et al. 2013, 2015; Gallenne 2015). The second point is more challenging because detecting and extracting radial velocities of the hot main-sequence companions from usual visible spectrograph is a difficult task due to the Cepheids brightness, blended lines and broad features (some companions are fast rotators). However, in the ultraviolet domain, the companion flux dominates the Cepheid, thanks to its early spectra type (~B5V), and the spectral disentangling is a lot easier. Our first results combining ultraviolet measurements from the Hubble Space Telescope (HST) with our interferometric orbit provided unprecedented results (see Fig. 2.1 and next paragraph). As a large survey of the brightest binary Cepheids with HST (a few tens of Cepheids) is difficult to obtain, such a survey with the Polish UV satellite would allow us to strongly enlarge our sample of dynamical masses and independent geometrical distances.

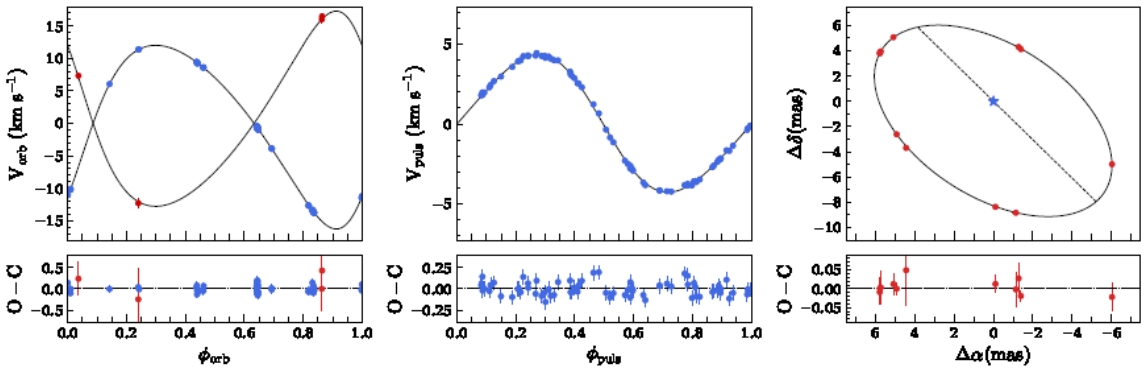

Figure 4.1: Left: fitted (solid line) and measured primary (blue) and secondary (red) orbital velocities. Middle: fitted and measured pulsation velocity. Right: orbit of V1334 Cyg Ab. The red dots are the MIRC astrometric points from 2012 to 2016, while the blue star denotes the Cepheid.

Cepheid Masses: Cepheids belonging to binary systems offer the opportunity of progress on the Cepheid mass problem. There is a disagreement between masses inferred from stellar pulsation and from stellar evolutionary models. By combining optical (from the ground) and ultraviolet (HST) spectroscopy with interferometric measurements, we are able to determine all the orbital elements, the distance, and the absolute masses of the two components, which will help us to understand the origin of this discrepancy. Recent works from Anderson et al. (2014) suggested that taking into account rotation and crossing number in the stellar evolution models remove this discrepancy, but accurate mass measurements are still necessary to test such models. So far, the mass of only one Galactic Cepheid has been dynamically measured (Evans et al. 2008). In Fig. 4.1, we present our new results of our observing program for the Cepheid V1334 Cyg. We combined our interferometric astrometry with optical and ultraviolet spectroscopy to measure the geometrical distance with an unprecedented accuracy of 1 %, together with
3% and 1% for the Cepheid and companion mass, respectively (Gallenne et al. 2018, in prep., hereafter G18). These are the most accurate distance and mass for a Galactic Cepheid. Note that this is the same accuracy level as the final stated GAIA astrometric performances.

Distance scale and the Hubble constant: The occurrence of Cepheids in binary systems seems to be at least 50%for the brightest Cepheids, and is often neglected in the determination of the P-L relation. The position of a Cepheid in this diagram could be biased by the presence of a close bright companion, which consequently, would bias its calibration, and therefore possibly the whole distance scale. By comparing our accurate distance of V1334 Cyg with current P-L relations, we showed that the companion has a significant impact on the integrated magnitude (G18). Correcting for the companion's flux brings the star closer to the position predicted by the P-L relations, with a stronger e_ect in V for this specific system. Recent works of Riess et al. (2016) used optical photometry of Cepheids from HST to derive a new calibration of the Hubble constantH0, but flux contamination from nearby companions is neglected. In G18 we computed a new calibration of the P-L relation based on direct distance measurements only, including our companion corrected measurement of V1334 Cyg, and rescaled H0 to 71.77 km s^{-1} Mpc^{-1}. We have reduced the current discrepancy with the Planck's results from 3.7 to 2.3σ. It seems therefore possible that the current tension between H0 predicted from the CMB fluctuations and the calibration using Cepheids is partly caused by photometric bias from nearby companions.
Note that the upcoming Gaia parallaxes of Galactic Cepheids promise to constrain the zero point of PL relations with high precision. But reddening corrections, biases from binarity (astrometric or photometric) and circumstellar envelopes will limit the true accuracy of the calibration if they are not properly taken into account.

5. Chromospheric activity of a nearby solar-like stars

Flares are the most extreme evidence of magnetic activity in stellar atmospheres. They are supposed to be the result of the energy release from magnetic field reconnection. In the classical scenario (Benz 2017) of the solar flare the reconnection occurs high in the solar corona. During that process streams of energetic particles are formed, and propagate down to the chromosphere. Along their path they exchange energy with surrounding plasma due to Coulomb collisions. After reaching the dense chromosphere the number of collisions grow abruptly due to rise of density. Particles thermalize eventually and heat lower parts of the solar atmosphere. Next, heated chromospheric plasma „evaporates" and fills up magnetic structures. The scenario is supported by various observables which may be adopted to the stellar observations. The aim is to answer the question: "How similar are stellar flares to the solar flares?".

5.1 Stellar flares

One of the most interesting is the region in the chromosphere, where energetic electrons lose their energy. It is well visible in the Hard X-ray, EUV and UV radiation during impulsive phase of solar flares. Observations of these ranges gave a lot of information about energy release and distribution in solar flares which may be extended to stellar flares. The behavior of different chromospheric lines during the flares will allow us to determine the physical parameters of the chromospheric flaring plasma (electron density and electron temperature), the temperature of the underlying source, and the surface area covered by the flaring plasma. We also will be able to search for possible relationships between the physical parameters of the flaring plasma and other properties such as the flare duration, area, maximum flux and released energy. Stellar flare monitoring requires high cadence observations (several minutes) through the few hours long observational window.

One of the well-recognized relation between physical parameters of solar flares is the Neupert effect which connects non-thermal radiation with derivative of thermal radiation. It is a consequence of the energy transport via non-thermal particle beam. The Neupert effect was observed in stellar flares (Güdel et al. 2002), but there is a lack of statistical analysis of it. If the Neupert effect is common for stellar flares then it may significantly supports the scenario in which the energy in the stellar flare is transported by streams of energetic particles. Connected to it is line asymmetry caused by the evaporation of chromospheric material. Observations of such effects may be the most demanding as they require cadence of 1 minute or shorter, and possible complementary X-ray observations.

5.2 Failed eruptions

The solar failed eruptions are one of many types of solar magnetic fields reconfiguration processes. Drivers of their confinement are unknown. Several mechanisms were proposed like too strong tethers, flux emergence complexity, kink instability leading to stable configuration of erupting flux tube, reconnection with magnetic field overlying the eruption site and others. Despite the confining mechanism we expect that energy of the failed eruption have to be distributed in the stellar atmosphere, and produce eventually enhancement of a radiation in various ranges of electromagnetic spectrum. One of possible stopping mechanism is the reconnection with overlying magnetic field (Amari & Luciani 1999) during which we expect streams of non-thermal particles which are produced and precipitated into denser parts of a stellar atmosphere. It has been found (Mrozek 2011) that such streams produce UV and EUVs sources

similar to solar flare footpoints. These sources give characteristic bumps in the decay part of a flare lightcurve (Netzel et al. 2012), and may be detected even for stellar flares.

Stellar failed eruptions may be more common as confining fields are much stronger than that observed in the Sun. Odert et al. (2017) estimated that critical energy for an eruptive flare could be a factor of 10^6 higher for an active star which is only 10^3 times more luminous in the X-ray range compared to the Sun. This means that only most energetic super flares may be accompanied by Coronal Mass Ejection on young solar-type stars. Therefore, the cosmic environment around planets revolving around such stars may be less harsh and more propitious for possible life on such planets.

5.3 Stellar activity cycles

Solar spectra irradiance variations are known to exhibit a strong wavelength dependence with amount of variability increasing towards shorter wavelengths. Solar flux variations in the UV range, from 115 to 220 nm, between solar activity maximum and minimum reaching 10% (Fligge et al. 2001). Active solar-like stars are expected to present similar or larger variations in this spectral range during there's activity cycle. Additionally, fast rotating stars activity cycles are expected to be shorter than 5 years (Saar & Brandenburg 1999), such sort cycles are within reach of the proposed experiment.

The mechanism driving solar and stellar activity cycles is still poorly understood and models of the solar and stellar dynamo lacking precision and possibly different models have to apply to different stars. Some authors have studied possible trends involving the activity cycle duration and its relation to other stellar parameters, e.g. stars may lie on three branches when the ratio of their cycle frequency to the angular rotational frequency is plotted against inverse Rossby number (Brandenburg et al., 1998; Saar & Brandenburg, 1999), these branches are called the inactive, active and superactive. It is thought that the different branches may be a manifestation of changes in the underlying dynamos of these stars as they evolve over their lifetime (Oláh et al. 2016). Additionally, stars lying along different branches exhibit different temporal chromospheric variations (See et al. 2016), this suggest different frequency and possibly morphology of the flaring activity, but the question: "How the flare activity differs on a stars lying on a different branches?" is still open. Activity monitored frequently (every few months) by obtaining Hi-resolution UV spectra of active solar-like stars laying on different activity branches over entire duration of the mission may contribute to answering this question.

6. Active Galactic Nuclei spectroscopy with UVSat

UVSat will be very valuable tool in study of the nature of Active Galactic Nuclei (AGN). UV is the prominent energy band where significant part of electromagnetic radiation is emitted. UV AGN spectra are also full of spectral details – emission and absorption lines – and their knowledge is an excellent diagnostic tools. AGN emit in the very broad energy band, from radio till X-rays, and the key supplementing information can be obtained in other spectral windows with instruments like ALMA or CHANDRA. However, the UV band frequently dominates energetically, and leads in time variability with other wavelength bands to follow. What is more, UV observations done for nearby sources can be linked directly to observations of high redshift AGN in the optical band, which are the subject of extensive ground-based survey and monitoring studies.
UV spectroscopy of AGN had been undertaken in the past with IUE, and currently HST, Swift and Astrosat. IUE measured spectra for a few dozen of active galaxies and successfully

performed a monitoring of 6 objects. UVSat will allow to add higher resolution observations thus expanding the list of possible goals, will increase a number of sources available for monitoring. What is also important, some AGN show surprising changes in their spectra over years (so called changing-look AGN; e.g. Mkn 335) so even reobserving the same object is of key importance. HST can devote only a very limited time to AGN, and Astrosat has very limited spectral resolution.

6.1 Broad-band spectral modeling, time-dependent irradiation effects

Since the AGN spectra most frequently peak in UV having a UV coverage allows to fit models of accretion disc spectra to the data. This is possible for both low redshift and moderate redshift sources. This allows directly constraint global parameters of black hole and its fueling mechanism (i.e. Czerny et al. 2011, Laor & Davis 2011, Calderone et al. 2013). In connection with ground base optical spectroscopy it will be possible to construct single epoch broad band spectrum. Spectrum in contrary to photometry will allow to take into count various emission lines contribution in great details, and thus describe the disc shape better, including the effect of illumination of the accretion disc. Illumination modifies temperature radial distribution resulting in local modification in accretion disc spectrum i.e. brightening in spectral windows which propagates toward longer wavelength over time (color correction, hardening factor). Thus repeating observations few times we will be able to describe evolution of the effect. This means deriving geometry of the disc surface and testing prediction from the simulations, where it was suggested significant departures from flat surface (Hryniewicz et al. 2013, Różańska et al. 2014, Adhikari et al. 2018). The observations of low redshift AGN in UV band has clear advantage over observations of moderate-z objects in optical band: they are systematically less massive thus the evolution time scale is much shorter - days rather than months, thus brings results much faster. Important product of joint observations: optical, UV and X-rays is spectral energy distribution (SED) this shows us how ionizing continuum in a given source may look like. This kind of information is necessary to conduct photoionization simulations which helps explain emission line spectrum. Although the selected sources are the closest AGN for many of them no UV spectra are available so far.

6.2 Structure and metallicity of the BLR

The kinematics of the BLR is still under debate, the Keplerian motion dominates, but the deviations in the form of inflow and outflow are under debate. Prominent broad emission lines in UV in contrary to visual band for nearby AGN covers both low ionization lines (LIL) and high ionization lines (HIL). Both of line species are produced in the UV + X-rays radiation field above accretion disc most probably in the outflows from accretion disc. However LIL and HIL are created in different conditions thus probably in distinct media in different locations (i.e. Collin-Souffrin et al. 1988, Czerny & Hryniewicz 2011). Apart from that, in lines two kinematic components are usually visible: broad component (BLR) and separate narrow component (NLR), with the second one coming from distances larger than the inner region of the dusty torus. Measurement of emission line flux allows to properly constrain physical conditions in the photoionized gas derived from the simulations (Baldwin et al. 1995, Leighly et al. 2007). However from the simulations emerge a new picture that smooth distribution of gas may be present above the accretion disc across broad radial range (Adhikari et al. 2017, 2018). This model explains presence of previously not well studied intermediate lines (kinematic broadening ~2000 km/s) in addition to broad (>4000 km/s) and narrow lines (~500 km/s). This model may be tested and tuned only with spectroscopy (resolution R >2900) and detailed study of spectral profiles of emission lines. Importance of UV band is supported by the ionization potential coverage in the emission lines, thus we would like to observe with UVSat given lines: Lyalpha

121.6 nm, N V 123.9 nm, 124.3 nm, Si IV 139.4 nm, 140.3 nm, C IV 154.8 nm, 155.1 nm, He II 164 nm, O III] 166.1 nm, 166.6 nm, N III] 175 nm, Al III 185.5 nm, 186.3 nm, Si III] 189.2 nm, C III] 190.9 nm, N II] 214 nm. Since part of those lines belong to semi-forbiden line group they have moderate critical density (n_H ~ 7-11 cm^{-3}) thus are perfect tool to probe density of the emitting medium. Decomposition of observed lines will allow also constrain geometry of the emitting medium and the intrinsic kinematics of gas (Kollatschny & Zetzl 2013, Czerny et al. 2017) and presence and influence of dust (Netzer & Laor 1993, Adhikari et al. 2016, Czerny et al. 2017). Spectral lines present in the FUV range such as N V 123.9 nm, 124.3 nm, C IV 154.8 nm, 155.1 nm, O III] 166.1 nm, 166.6 nm, N III] 175 nm allows also to derive metallicity of the accreting matter (Hamann et al. 2002). With derived metallicity we will fix one of the most important free parameter of the model of BLR and we will verify the assumption about solar like abundance often used in simulations.

6.3 Monitoring campaigns and black hole mass determination

Black hole mass measurement is of a key importance for AGN themselves and for cosmological studies of the galaxy evolution. Key method used in massive surveys is based on observationally derived relation between the black hole mass, the line kinematic width, and the source monochromatic flux. Such a law is obtained from monitoring campaigns of several sources, and the measurement of the time delay between the line and the continuum which serves as a proxy for the BLR radius. Such measurements were done for about 70 sources by now but mostly for Hbeta (486.1 nm) line and the corresponding 510 nm continuum. With UVSat we propose to do reverberation in C IV (154.8 nm, 155.1 nm) line for selected sources. For these lines only a few measurements are available so far, and this lines are the only one available in the optical band for the majority of (large redshift) quasars. Thus observing nearby AGN in UV will allow us to calibrate BH mass derivation in more distant sources. This will allow to have better estimations of BH masses on z > 1 from currently available and future optical spectra of distant quasars. Selecting sources we concentrated on those which were previously a subject of ground-based monitoring campaign in Hβ, so having needed supplementary information.

6.4 Absorption features and the AGN outflows

Outflows in AGN carry an amount of mass which is likely a significant fraction of the accreting flow, and this can easily affect the host galaxy through the feedback mechanism. This outflow is visible in the data as UV and X-ray absorption features, and the features show frequently (but not always) an overlap in terms of velocity. In ~50 % of the sources noticeable narrow absorption lines (NAL) are present. Absorption allows to study gas distributed along the line of sight across AGN and its host galaxy. It was already suggested based on observations of Mrk 509 and NGC 5548 that gas is present across ionization parameter scale (log xi: -8.5 - 3.5; Detmers et al. 2011, Steenbrugge et al. 2011) and part of absorbing gas overlaps with broad emission lines region (Kaastra et al. 2011). NAL in the UV range effectively probe low ionization parameter space xi < 10 (Kriss et al. 2011). This allows to better constrain absorption measure distribution (Holczer et al. 2007, Adhikari et al. 2015) in the low xi regime.

6.5 The properties of the host galaxies in selected AGN

In most type 1 AGN UV is dominated by an AGN, but for Seyfert 2 galaxies or Low Luminosity AGN the starlight contribution dominated the UV. This, combined with high spectra resolution, would allow the detailed study of the stellar content. This is important for AGN SED studies in general, since UV study will show the likely presence of the young stellar population in these

galaxies, in analogy to the nuclear stellar cluster of Sgr A*. In typical SED studies the stellar template used usually consists of old stars only, which may affect the broad band SED fitting.

7. Cometary spectroscopy with UVSat

Comets formed about 4.5 billion years ago, i.e., at the very beginning of the Solar System. They emerged in the protoplanetary disk from leftover material from the formation of Sun and planets. Because the matter contained within these objects has not undergone significant changes since that time, they are extremely valuable to science, acting as unique "time capsules" that contain precious information from this bygone age.

The FUV range enables the observation of several emission lines and bands that are of a fundamental importance to cometary astrophysics, most notably:

- the Lyman α hydrogen line at 1216 Å,
- the *Fourth Positive Group* of CO between 1320 and 1750 Å,
- the forbidden CO bands from the *Cameron system* between 1910 and 2220 Å.

The growing interest in these lines and bands – especially when they are observed simultaneously – stems from the fact that they allow to determine the abundances of three most significant non-organic components of cometary ice, i.e., H_2O, CO_2, and CO, which bear the footprints of the physical and chemical conditions in which comets formed and their subsequent thermal evolution. To date, the abundances of all three molecules have only been measured for ~10 comets (A'Hearn et al. 2012, ApJ 758, 29), and probably for none of them truly simultaneously and from the same region around the comet's nucleus. The planned UVSat observations will offer a breakthrough in terms of measurement consistency and will dramatically increase the sample of targets investigated in this way – by an order of magnitude during the expected 10-yr mission lifetime. Thus, results from this program will be transformative for cometary science.

The excellent sensitivity of UVSat will allow us to obtain routine measurements of H_2O, CO_2, and CO for ~10 comets per year. Our nominal observing strategy will be to take ultra-deep spectra of selected targets in one go. Given the importance and rarity of such measurements, each investigated target will deserve a separate publication in a recognized peer-reviewed journal. Exceptionally bright comets – much brighter at peak brightness than the detection limits given below – will be observed on multiple occasions. This will allow us to trace the relative abundances of the aforementioned volatiles over extended periods of time and in this way address the unresolved problem of their observed uncorrelated behaviors (e.g. Feaga et al. 2014, AJ 147, 24). Special attention will be paid to bright comets that undergo outbursts and breakups, as these bodies offer unique insights into the matter excavated from deep in their interiors. The targets will normally be selected anywhere from weeks to years before the observations, but in exceptional circumstances (e.g. outbursts) it will be desirable to trigger observations within hours. The selection will be based on observed or predicted total visual brightness, monitored nightly for dozens of comets by amateur astronomers, and on geocentric distance.

The UV range would allow for a comfortable measurement of these molecules using the aforementioned emission bands. The H_2O sublimation rate can be determined from the hydrogen content, which is easy to measure using the intensity of the Lyman α line. In turn, the CO_2 sublimation rate can be determined through the observation of the forbidden CO bands that form the *Cameron system* (Figure 5.1, bottom), which become excited during the formation of CO from the photodissociation of CO_2 in the cometary atmosphere. The total production rate of CO (i.e., both sublimating from cometary ice and created by the photodissociation of CO_2) can be determined using the *Fourth Positive Group* of CO (Figure 5.1, top). These methods in combination allow us to obtain the sought sublimation rates of H_2O, CO_2, and CO.

While cometary H_2O and CO can be measured from the ground, the CO_2 molecule absolutely requires extraatmospheric observations (indirectly, through the aforementioned *Cameron system* of CO in the UV, or directly, through the strong vibrational band ν_3 in the IR), which is why it has so far

seldom been observed. Consequently, the greatest value of the proposed spectroscopic observations of comets with UVSat lies in the possibility of indirectly detecting CO_2. The *Cameron bands* were first detected in the cometary spectrum using HST in 1991 during the observations of the 8-th magnitude comet 103P/Hartley 2 (Weaver et al. 1994, ApJ 422, 374), and were subsequently detected in the archival spectra of four much brighter comets, obtained with IUE. The greatest challenge, however, is to detect the *Fourth Positive Group* (FWHM of 5 Å). While the bands forming the *Cameron system* are some 0.3 mag fainter, they are also broader (FWHM from 15 to 20 Å), thus allowing for a more aggressive binning, resulting in a sensitivity advantage of about 0.5 mag. The Lyman α line, on the other hand, will be easiest to detect in spite of its very narrow profile, the width of which depending on the velocity of hydrogen atoms in the cometary atmosphere and being equal to about 30 km/s.

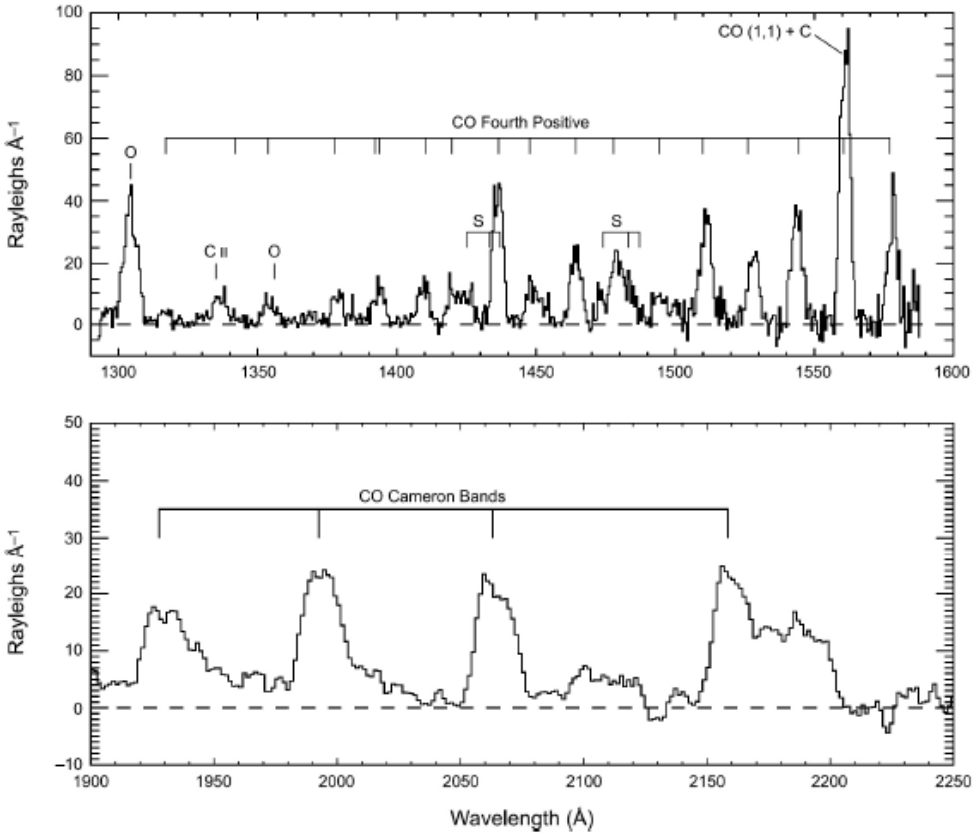

Fig. 7.1 Portions of the UV spectra of comet C/1996 B2 (Hyakutake) taken on 1 April 1996 with the HST. Figure adapted from Bockelée-Morvan et al. (2004).

(FWHM of 5 Å). In turn, the high-resolution mode (R = 25,000) will be well suited to the observation of the Lyman α line, the width of which depends on the velocity of hydrogen atoms in the cometary atmosphere and is equal to about 30 km/s.

Groundbreaking research on comets can also be carried out in the photometric mode of UVSat, the implementation of which is extremely desirable from our perspective. The main potential of this mode lies in the capability of measuring changes in the rotation rates of active comets from short-term brightness variations.

8. Observability of different kind of sources by UVSat

8.1 Observability of the binary stars

About **40 classical novae (CNe)** per year are expected in MW but not all observed, e.g., in 2018, so far 9 novae have been detected in MW (21.04.2018) and one in the LMC (which has turned out to be a recurrent nova). A few CNe/yr are expected in the MCs; e.g., the nova rates of 2.4 ± 0.8 per year (LMC) and 0.9 ± 0.4 per year (SMC) were derived from OGLE data.
Another class of transients are all kinds of **supernovae** (SN), and one should expect that a few bright (nearby) SN will happen.
Currently, about **300 symbiotic stars (SySt)** are known in MW and about 20 in MCs, however much more are expected to be detected in the coming years by ongoing systematic surveys for these objects.
Evolved hot stars, **Wolf-Rayet (WR) stars**, luminous blue variables (LBV) and OB stars are very important testbed for massive star evolution. There are bright and could be easily observed even with a small aperture satellite. E.g., typical ST magnitude at 1500 A for WR stars in the MCs are m_{1500}~8-10. With longer exposure times (~10000 sec) they could be also reached in the Local Galaxy Group (LGG). There are about a few hundred known WRs in MW, MCs and LGG.

8.2 Observability of the Classical Cepheids

Potencjalnie mamy ok 20-30 dobrych układów w Galaktyce przy 30cm. Przy 50cm dwa razy tyle. Należy wykonać obserwacje w kwadraturach. Przy okresach rzędu roku można spodziewać się kilku obserwacji na miesiąc. Projekt jest super wydajny i łatwy, bo kwadratury długo trwają - jest czas aby zrobić kilka obserwacji. Kluczowe: aby moc zarejestrować składnik wtórny potrzebujemy UV. Bez tego mamy tylko funkcję mas, wiec masa rzeczywista Cefeid jest tylko oszacowana. Mierząc prędkości składnika wtórnego możemy mierzyć masy z dokładnością rzędu 1% w Galaktyce. NUV: rozdzielczość wysoka. Czasy ekspozycji dość trudno oszacować: nie znamy stosunku jasności w tych układach podwójnych.

8.3 Observability of the chromospheric active stars

Targets availability using proposed 30 cm telescope: Chromospheres of bright ($M_v \leq 5$) nearby late type main sequence stars are well within reach of 30 cm UV telescope with spectra integration time no longer then several minutes. Based on observations of Mg II emission lines as stellar activity indicators of main sequence F-K stars (Buccino & Mauas 2008) we can estimate that at least several dozens of such active bright stars can be observed by the proposed instrument.

Observation campaign	Stellar activity cycles	Flares (confined/eruptive)
Number of available targets	~50 nearest K, G and F type stars.	~50 nearest K, G and F type stars.
Observation strategy	Monitoring the activity of stars throughout the duration of the mission. Once a year collecting about 20-30 spectra evenly distributed over several periods of target star rotation (10-50 days). Low spectral resolution.	"Aiming" into a flare. A few-hour monitoring of target star; cadence not longer than 5 minutes. Low spectral resolution.
Significance	Mechanisms generating solar and	Theoretical modeling shows that the

	stellar cycles are still an poorly understood area of astrophysics. Stellar chromospheres observations indicate that solar-like stars activity cycles properties can be divided into inactive, active or superactive group. It is thought that the different groups may be a manifestation of changes in the underlying dynamos of those stars as they evolve over their lifetime, but the question: "How the flare activity differs on a stars belonging to different groups?" is still open.	magnetic fields in coronas of active late spectral type stars can be so strong that virtually all ongoing coronal mass ejections (CMEs) are stopped and do not propagate into interplanetary space. Such events are called confined flares. Currently, there is no technical possibility to directly observe CME on other than Sun stars, but we are able to follow the so-called late phase of the flare in the FUV range. Confined phenomena are characterized by a long-lasting increase of brightness in the UV range associated with the lack of brightness in the x-ray range. Additionally the UV brightness exceeds the brightness during the impulsive phase of the flare. Observations of this effect in the case of stellar flares would allow for quantitative analysis of the interplanetary space condition and its possible impact on extrasolar planets around active stars.
Preferred spectral range	NUV or FUV Integration time: few minutes	FUV Integration time: <=5min

8.4 Observability of the AGN sources

In estimation of the observability prospects, we assumed the integration time of 10 000 s and S/N = 20 at least for NUV band. The Appendix 1 list 122 observable sources selected by its archival data from GALEX photometry. Not all sources have FUV measurements because of breakage of GALEX FUV detector since when only NUV observations were conducted. Those sources were marked with "P" as at least partly observed which means that we would achieve S/N = 20 at least for NUV, but in most such cases in AGN due to the usual shape of the unabsorbed spectral continuum we expect also high signal in FUV band. There are 150 more sources, not listed here, which are known to have NUV flux level above the assumed level for 50 cm telescope but with FUV level known to be below assumed here. Those additional sources are also partly observable but with lower prospects.

8.5 Observability of the comets

Taking the IUE measurements of comet Halley (Feldman et al. 1997, ApJ 475, 829) as a working example, we calculated UVSat's sensitivity to the *Fourth Positive Group* of CO for a comet Halley analog with $CO_2/H_2O = CO/H_2O = 6\%$ observed at 1 AU from the Sun. Note that for some comets the CO_2 and CO abundances significantly exceed 10%, making the choice of the composition of comet Halley a moderately conservative one. In Figures 1 and 2 we present the lines of a constant integration

time (or ST magnitude) as functions of the total visual magnitude and geocentric distance, calculated for S/N = 10 and R = 3000 with 10x binning.

1.

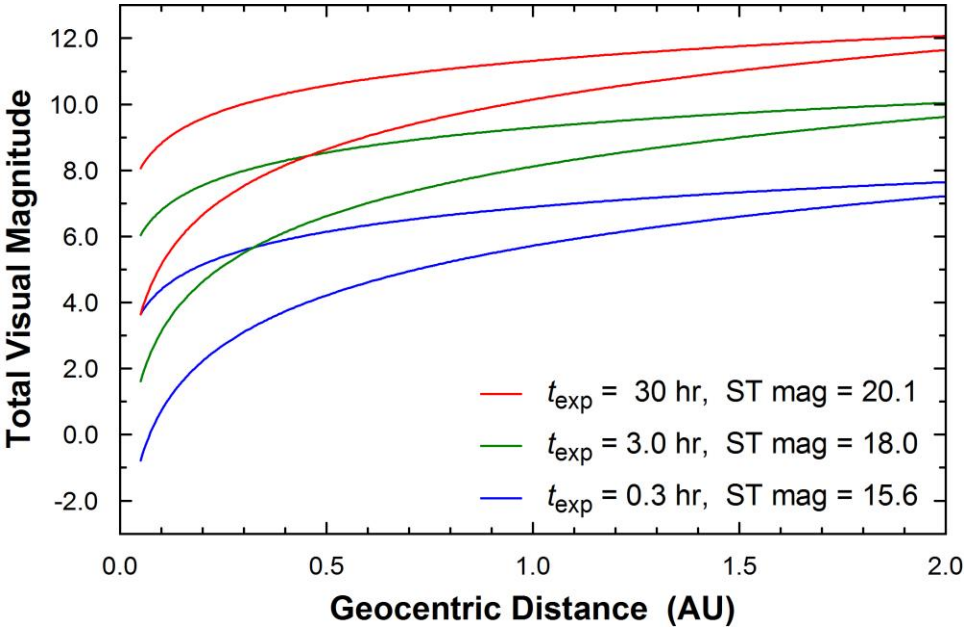

Figure 8.1. Sensitivity curves for 30 cm diameter mirror. For each integration time two curves are presented for extreme surface brightness profiles.

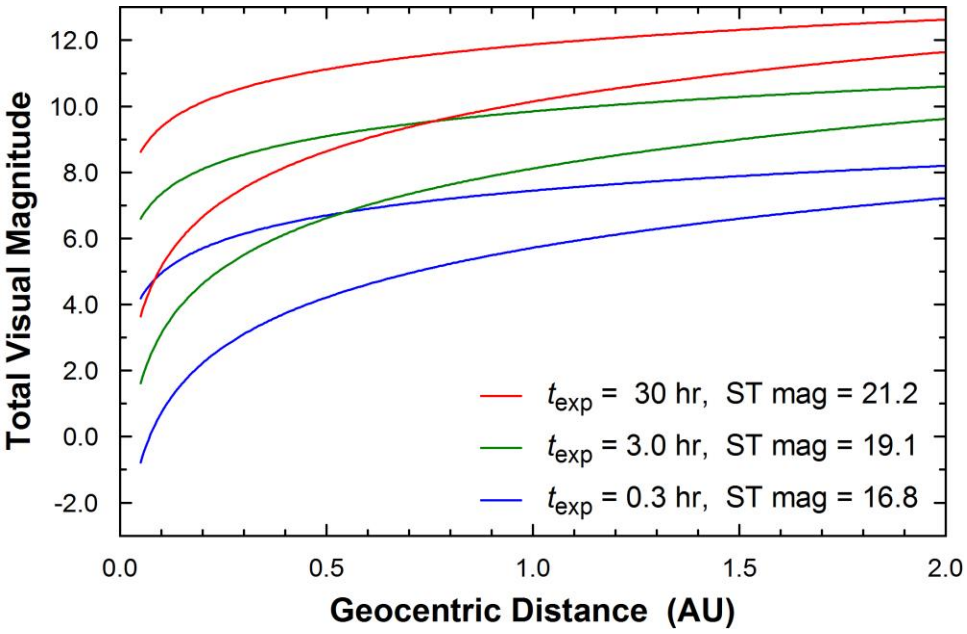

Figure 8.2. Sensitivity curves for 50 cm diameter mirror. For each integration time two curves are presented for extreme surface brightness profiles.

The figures demonstrate an excellent sensitivity of UVSat, which will be able to detect the most interesting cometary lines and bands in the UV for comets down to ~12-12.5 mag in total visual brightness. Such comets are available essentially at all times, and their rate is ~10 per year. The

figures also show an ST mag sensitivity advantage of the larger UVSat version (mirror diameter of 50 cm) over the smaller one (30 cm mirror) of ~1.1 mag. However, for a given total visual magnitude and geocentric distance, cometary emission bands in ST mag will actually be brighter by ~0.55 to ~1.1 mag (depending on the assumed surface brightness profile) when observed through the smaller, 30 cm telescope, thanks to a larger projected slit compared to the 50 cm telescope. The net sensitivity advantage of the larger telescope in total visual brightness is then up to ~0.55 mag. Additional sensitivity improvement can be achieved by using a long slit, which – for brighter targets – will also provide valuable information about spatial distribution of the observed molecules.

References

Adhikari, T. P. et al., 2015, ApJ, **815**, 83
Adhikari, T. P. et al., 2016, ApJ, **831**, 68
Adhikari, T. P. et al., 2018, ApJ, **856**, 78
A'Hearn et al. 2012, ApJ, **758**, 29
Amari, T. & Luciani, J.F., 1999, ApJ, **515**, L81
Anderson, R. I., Ekström, S., Georgy, C., et al. 2014, AA, **564**, A100
Baldwin, J. et al., 1995, ApJ, **455**, L119,
Benz, A.O. 2017, Living Rev. Sol. Phys. 14:2
Bockelée-Morvan et al., 2004, in: Comets II, p. 391.
Boggess, A., Carr, F.A., Evans, D.C. et al. 1978, Nature, **275,** 372
Brandenburg, A., Saar, S. H., & Turpin, C. R. 1998, ApJ, **498**, L51
Buccino & Mauas 2008, Astronomy & Astrophysics 483, 903
Calderone, G. et al., 2013, MNRAS, **431**, 210
Collin-Souffrin, S. et al., 1988, MNRAS, **232**, 539
Czerny, B. et al., 2017, ApJ, **846**, 154
Czerny, B. & Hryniewicz, K., 2011, A&A, **525**, L8
Detmers, R. G. et al., 2011, AA, **534**, 38
DiStefano, R., 2010, ApJ, **719**, 474
Eaton, J.A. 2016, MNRAS, **457**, 836
Eaton, J.A, Wu, C-C., & Rucinski, S.M. 1980, ApJ, **239**, 919
Evans, N. R., Schaefer, G. H., Bond, H. E., et al. 2008, AJ, **136**, 1137
Fleming, B.T., France, K., Nell, N., et al. 2018, arXiv:1801.02673v1 (astro-ph)
Fligge, M., Solanki, S. K., Pap, J. M. et al. 2001, Journal of Atmospheric and Solar-Terrestrial Physics, **63**, 1479
Gallenne, A. 2015, in RMxAC Conference Series: VI Reuni´on de Astronom´ıa Din´amica en Latinoam´erica (ADeLA 2014), Vol. **46**, 32
Gallenne, A., M´erand, A., Kervella, P., et al. 2015, A&A, **579**, A68
Gomez de Castro, A. I., 2014, https://arxiv.org/pdf/1306.3358.pdf
Green, J.C., Froning, C.S., Osterman, S. et al. 2012, AJ., **744**, 60
Güdel, M., Audard, M., Smith, K.W. et al., 2002, ApJ, **577**, 371
Hamann, F. et al., 2002, ApJ, **564**, 592
Hasinger, G., Turner, M. J. L., Proc. SPIE 5488, 0277-786X/04Hutchings, J.B. 2014, ASS, **354**, 143
Hendry, P. D., & Mochnacki, S. W. 2000, ApJ, **531**, 467
Holczer, T. et al., 2007, ApJ, **663**, 799
Hryniewicz, K. et al., 2012, J. Phys.: Conf. Ser., 372, 012060
Kaastra, J. S. et al., 2011, AA, **534**, 37
Kollatschny, W. & Zetzl, M., 2013, AA, **549**, 100
Kriss, G. A. et al., 2011, A&A, **534**, 41
Laor, A. & Davis, S. W., 2011, MNRAS, **417**, 681
Leighly, K. M. et al., 2007, ApJS, **173**, L1

Lira, P. et al., 2018, Front. Astron. Space Sci., 4:71,
Lucy L. B., 1968a, ApJ, **151**, 1123
Lucy L. B., 1968b, ApJ, **153**, 977
Mikołajewska, J., 2013, in Binary Paths to Type Ia Supernovae Explosions (IAU S281), eds. R. Di Stefano, M. Orio, M. Moe, Cambridge U. Press, p. 162
Mikołajewska, J., Shara, M.M., 2017, ApJ, **847**, 99
Mochnacki, S.W. and Doughty, N.A. 1972, MNRAS, **156**, 51
Molaro, P., Izzo, L., Mason, E., Bonifacio, P., Della Valle, M., 2016, MNRAS, **463**, L117
Mrozek, T. 2011, Solar Physics, **270**, 191
Murthy, J., Henry,R.C. and Sujatha, N.V. 2000, ApJ, **724**, 1389.
Netzer, H. & Laor, A., 1993, ApJ, **404**, L51
Netzel, A., Mrozek, T., Kołomański, S. & Gburek, S., 2012, AA, **548**, A89
Odert, P., Leitzinger, M., Hanslmeier, A. & Lammer, H., 2017, MNRAS, **472**, 876
Oláh, K. Kővári, Zs. Petrovay, K. Soon, W. et al., 2016, AA, **590**, 133
Paczyński, B. 1964, AJ, **69**, 124
Pribulla, T., Rucinski S. M., 2008, MNRAS, **386**, 377
Różańska, A. et al., 2014, NewA, **28**, 70
Rucinski, S.M. 2015, AJ, **146**, 49
Saar, S. H. & Brandenburg, A., 1999, ApJ, **524**, 295
Sahnow, D. et al. 2000, Proc. SPIE 4013, p. 334-343
Scott, A., et al. 2014, Proc. SPIE 9154, 91542C-1
See, V., Jardine, M., Vidotto, A. A., et al., 2016, MNRAS, **462**, 4442
Shen, Y. et al., 2016, ApJ, **818**, 30
Shen, Y. et al., 2016, Astron. Soc. Pac. Conf. Ser., **507**, 367
Siegmund, O. et al. 1997, Proc. SPIE Vol. 3114, p. 283-294
Siegmund, O. et al. 2004, in "UV and Gamma-Ray Space Telescope Systems, edited by
Smith, L.J., Willis, A.J., 1993, A&AS, **54**, 229
Stahl, H. Philiip, et al. 2010, SPIE 7731, 77312N
Steenbrugge, K. C. et al., 2011, AA, **534**, 42
Weaver et al. 1994, ApJ, **422**, 374
Woodgate, B.E., Kimble, R.A., Bowers, C.W., et al. 1998, PASP, **110**, 1183